

Generative Design by Reinforcement Learning: Maximizing Diversity of Topology Optimized Designs

Seowoo Jang

Department of Electrical and Computer Engineering

Seoul National University

sjang@netlab.ac.kr

Namwoo Kang^{*}

²Department of Mechanical Systems Engineering

Sookmyung Women's University

nwkang@sm.ac.kr

^{*}Corresponding author

Abstract

Generative design is a design exploration process in which a large number of structurally optimal designs are generated in parallel by diversifying parameters of the topology optimization while fulfilling certain constraints. Recently, data-driven generative design has gained much attention due to its integration with artificial intelligence (AI) technologies. When generating new designs through a generative approach, one of the important evaluation factors is diversity. In general, the problem definition of topology optimization is diversified by varying the force and boundary conditions, and the diversity of the generated designs is influenced by such parameter combinations. This study proposes a reinforcement learning (RL) based generative design process with reward functions maximizing the diversity of the designs. We formulate the generative design as a sequential problem of finding optimal parameter level values according to a given initial design. Proximal Policy Optimization (PPO) was applied as the learning framework, which is demonstrated in the case study of an automotive wheel design problem. This study also proposes the use of a deep neural network to instantly generate new designs without the topology optimization process, thus reducing the large computational burdens required by reinforcement learning. We show that RL-based generative design produces a large number of diverse designs within a short inference time by exploiting GPU in a fully automated manner. It is different from the previous approach using CPU which takes much more processing time and involving human intervention.

Keywords: Generative Design, Topology Optimization, Deep Learning, Reinforcement Learning, Design Diversity Maximization

1. Introduction

The recent advent of deep learning has introduced new methods for tackling problems previously considered intractable or not addressable because of their highly nonlinear nature or complexity. The outstanding success in image and voice recognition has proven that artificial neural networks can achieve or even surpass human-level performance in a given field (Kirillov et al., 2019; Krizhevsky et al., 2012; Sutskever et al., 2014; Vaswani et al., 2017). With the help of big data and ubiquitous computing power to process them, neural networks are capable of approximating or capturing nonlinear relations hidden within the problems and they are at the core of the success. The power of approximation imbues the neural network to generalize to inputs previously unseen during training.

However, as previously mentioned, deep learning techniques require a huge amount of data for the neural network to find the non-linear relations or hidden probability distribution of the problem within the target data. This requirement sometimes restricts the application of this approach where data are difficult or expensive to acquire. In such areas, reinforcement learning (RL) (Sutton & Barto, 2018), in which the training agent learns how to act through interaction with an environment, is considered a promising methodology.

In computational design, extensive research has been conducted regarding deep learning in fields such as design optimization (e.g., size/shape/topology optimization), computer-aided design (CAD), computer-aided manufacturing (CAM), computer-aided engineering (CAE), and meta-modeling, among others (Yoo et al., 2020). In particular, topology optimization is a research field that actively applies machine learning and deep learning (Lin & Lin, 2005; Sosnovik & Oseledets, 2017; Keshavarzzadeh et al., 2020; Roux et al., 2020). By definition, topology optimization is a methodology to determine the optimal distribution of material in a design space, given a set of load and boundary conditions. Since the material density is similar to the concept of image pixels, deep learning models based on convolutional neural networks (CNNs) and generative adversarial networks (GANs) have been applied actively (Banga et al., 2018; Oh et al., 2018; Yu et al., 2019; Oh et al., 2019).

On the other hand, generative design is a technique that uses topology optimization to explore numerous new designs. Oh et al. (2019) proposed a deep learning-based generative design process that can create aesthetic as well as engineered designs utilizing reference design data in the market. The key idea of generative design is to create various optimal structural designs by varying the design parameters that define a topology optimization problem. Therefore, the diversity of the generated designs is affected by the combinations of the design parameters such as volume fraction, force, and boundary conditions, among others. Previous approach has determined parameter combinations based on the designer's hunch coming from experience and then verify the design through computation. However, design diversity is the most important characteristic of generative design to be optimized thus requires an automated approach in large-scale that generalizes to unseen inputs.

This study proposes an RL-based generative design framework that can maximize the diversity of generated designs. The proposed framework can immediately present a set of optimized design parameter combinations based on a given reference design for maximizing the design diversity. A recent study (Sun and Ma, 2020) also applied RL to improve iterative design exploration without varying the problem definition, yet this approach does not guarantee maximum diversity and aesthetics. We focused on developing two neural networks as the main part of the proposed RL framework: one to approximate the topology optimization process, named TopOpNet, and another to find a combination of design parameters leading to maximum diversity, GDNet.

First, we exploit the universal function approximation characteristic of neural networks to perform the highly nonlinear and complex operation of a conventional topology optimization algorithm. This is carried out by TopOpNet, our proposed neural network that, with a limited amount of data, achieves results similar to those of the conventional algorithm, or even better in the cases when the algorithm fails to maintain symmetric consistency.

Second, on top of the TopOpNet, taking advantage of the reduction in computation time, we suggest a novel approach of using the RL framework to define the optimization problem, which we call GDNet. There are previous works in the literature that apply RL when designing the engineering structure of an apparatus in a fully automated manner (Li & Malik, 2016; Yonekura & Hattori, 2019; Ha, 2019). In conjunction with virtual simulation based on real-world restrictions, previous works show the feasibility of RL to design structures that meet engineering requirements. In contrast, the present work focuses on applying RL to suggest design candidates as diverse as possible while fulfilling the physical requirements. To achieve this goal, we address the maximum design diversity problem with neural networks.

Fig. 1 shows the entire process of our work. As shown in the figure, we first run the conventional topology optimization algorithm to generate training data. Then, TopOpNet is trained with the pre-generated data to achieve well-approximated neural models that provide generalized performance on unseen inputs with much less computation time and power. In addition, we propose a reinforcement learning framework that uses the significantly reduced optimization time of TopOpNet. The trained model, GDNet, is shown to produce a set of topologically optimized designs with maximum diversity. We believe that wide diversity in design can help reduce the efforts and ingenious thinking required to obtain generic designs.

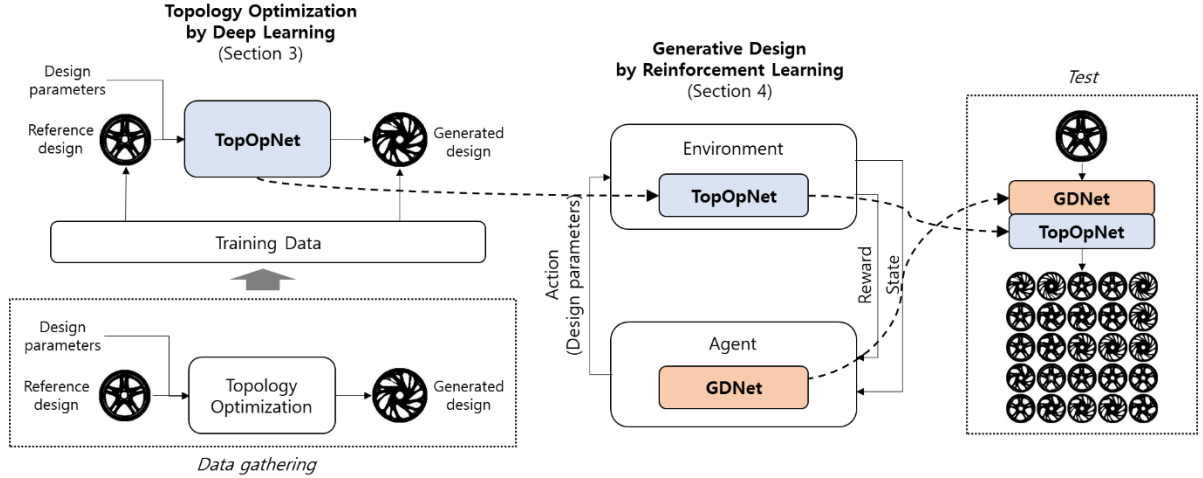


Figure 1. Research framework: reinforcement learning with TopOpNet and GDNet.

The contributions of this paper are as follows:

- We propose two TopOpNet architectures with the generalization performance of producing similar-to-algorithm results (and even better in some cases) for unseen inputs. The results can be achieved in much less time and with much less computational power compared to the iterative topology optimization algorithm. The details are given in Section 3.
- We present a novel approach for using RL for the maximum design diversity problem. We find that the problem has a non-trivial solution so that deep learning is a suitable choice for solving it. The problem is formulated as a sequence of parameter selection stages based on RL rewards. Design choices for the reward function, neural network architecture, and RL framework are presented in detail in Section 4.
- We demonstrate the feasibility of using RL for an automotive wheel design problem, which opens up new applications of RL in the engineering design domain.

The remainder of this paper is organized as follows. In Section 2, we provide a preliminary background for generative design, deep learning architectures, and reinforcement learning. In Section 3, we present TopOpNet with details on the neural network architecture and the results. Then, we elaborate on the GDNet, which generates the maximum diversity of designs that satisfy physical constraints in Section 4. Finally, concluding remarks and future works are given in Section 5.

2. Background

In this section, we provide preliminary background for generative design, deep learning architecture, and reinforcement learning, which constitute the baselines for our problem.

2.1 Topology Optimization and Generative Design

The terms topology optimization and generative design are often used interchangeably. However, in this study, the two methodologies are distinguished as follows. Topology optimization is a conventional structure design optimization technique. It uses the finite element method (FEM) to determine the material density of elements and finds the optimal structural layout to maximize engineering performance (typically minimize compliance) under given load and boundary conditions (Andreassen et al., 2011). The topology optimization problem can be

defined differently depending on the designer or environment, and a different optimal design can be obtained according to the problem definition.

Generative design is a technique that utilizes topology optimization to create numerous structure designs by varying the topology optimization problem definition. Designers can discretize the design parameters used in the topology optimization algorithm and execute topology optimization for each set of design parameter values using parallel computing. Oh et al. (2019) proposed a generative design formulation to create a structural design that has high stiffness and is similar to the target reference design. This method allows designers to create aesthetic and engineering designs. The formulation is:

$$\begin{aligned} \min \quad & f(\mathbf{x}) = \mathbf{U}^T \mathbf{K}(\mathbf{x}) \mathbf{U} + \lambda \|\mathbf{x}_r - \mathbf{x}\|_1 \\ \text{s. t.} \quad & \frac{V(\mathbf{x})}{V_0} = R \\ & \mathbf{KU} = \mathbf{F} \\ & 0 \leq x_e \leq 1, \quad e = 1, \dots, N_e. \end{aligned} \quad (1)$$

This is a multi-objective optimization problem that minimizes compliance, $\mathbf{U}^T \mathbf{K}(\mathbf{x}) \mathbf{U}$, and minimizes the distance between the target reference design and the generated design, $\|\mathbf{x}_r - \mathbf{x}\|_1$. The design variables used are: \mathbf{U} as the displacement vector, \mathbf{K} as the global stiffness matrix, \mathbf{F} as the force vector, and \mathbf{x} as the density vector of the element. If x is 1, the element is completely filled, and if x is 0, the element becomes empty. The L1 norm is used for the distance between designs, and similarity weight λ controls the tradeoff between compliance and similarity to the reference design. As an equality constraint, R is the volume fraction, where $V(\mathbf{x})$ is the volume of the generated design, and V_0 is the volume of the reference design.

To create a variety of designs, designers can change the design parameters used in Eq. (1). For example, after discretizing the similarity weight λ and changing from small to large, designers can create designs that are very similar to the reference design, as well as designs that are very different from the reference design.

This study uses the wheel design problem of Oh et al. (2019) to demonstrate the proposed RL framework. We chose two design parameters: force ratio (i.e., the ratio between normal force and shear force) and similarity weight. In previous studies, the design parameter values were chosen at equal intervals between the minimum and maximum values, as shown in Fig. 2. The purpose of our study is to select optimal design parameter combinations according to reference designs to maximize the generated design diversity. We assume that the optimal design parameter combinations depend on the reference design, and that there are no trivial optimal points.

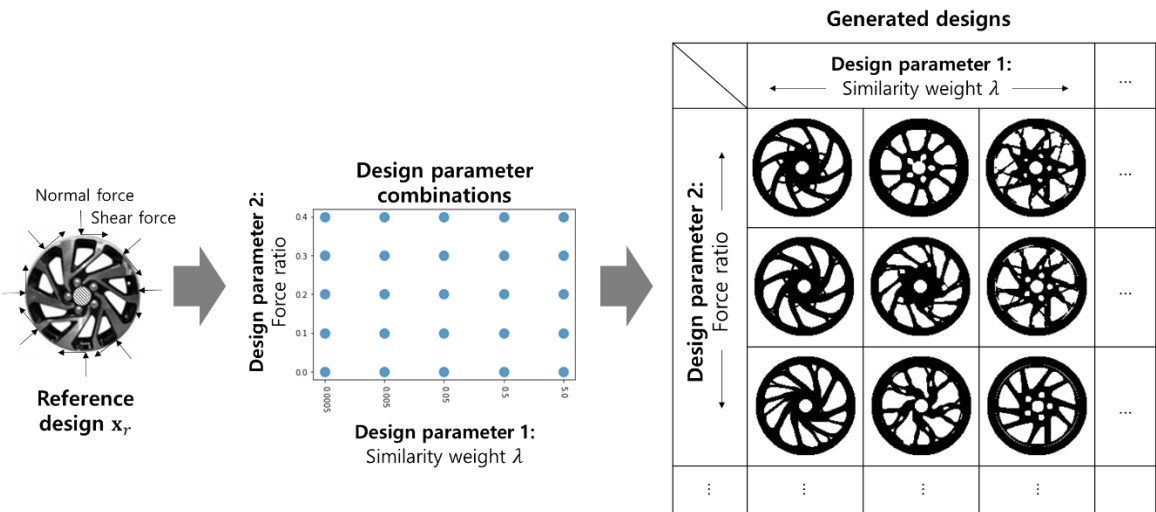


Figure 2. Generative wheel design problem

2.2 Deep Neural Network Architectures

There are three problems mainly addressed in learning-based visual data processing: image classification, object detection, and semantic segmentation. As this work is highly related to image classification and semantic segmentation, we briefly skim through some previous work on those fields.

ResNet (He et al., 2016) proposed to alleviate the vanishing gradient problem that limits the use of a deep neural network architecture for better feature extraction. In order to achieve this goal, ResNet adopted residual connections that directly connect inputs and outputs of a network block, thus letting gradients backpropagate directly. In addition, the residual connections help the network blocks learn only the difference in the feature space induced by the network block, resulting in more learning capacity. In addition, the authors used batch normalization to regularize the features between the network blocks in order to enhance feature extraction. Using these methods, ResNet achieved good performance in image classification problems by stacking up to 152 layers in the network.

On the other hand, Inception (Szegedy et al., 2015, 2017) addressed the same problem using a network-in-network architecture. Within a network block, 1×1 convolution layers were included to reduce the channel dimension of the input features, which resulted in feature encoding effects while matching the channel dimension with other feature maps. While stacking multiple network blocks, the authors attached auxiliary classifier branches in the middle of the network to enhance backpropagation from the output features. They achieved state-of-the-art performance with this new architecture for image classification problems.

In contrast, for semantic segmentation, a simple fully convolutional network (FCN) (Long et al, 2015) was proposed. Removing fully connected layers helped reduce the size of the network while matching the input/output characteristics of the semantic segmentation problem. The encoder-decoder architecture was used to extract features from input images and reconstruct a semantic map. During decoding, deconvolution layers were used for the reconstruction. To handle the gradient vanishing problem, the authors exploited skip layers connecting features from the encoder to the decoder.

DeepLab (Chen et al., 2017) also addressed the semantic segmentation problem by applying more advanced features on top of the FCN. To increase the size of the receptive field, Atrous spatial pyramid pooling (ASPP), a sequential network block with different dilation sizes, was used. The conditional random field (CRF) was incorporated within the decoding layers for better feature reconstruction.

We have referenced fundamental network architectures from previous works to implement a lightweight network architecture for our topology-optimized problem as a feature extractor. We elaborate the details later in this paper.

2.3 Reinforcement Learning

Unlike supervised learning, an RL agent learns how to act through interactions with an environment. RL is basically an extension of the Markov decision process (MDP), but does not require explicit models of the interacting environments. Through these interactions, the agent learns optimal actions in terms of long-term expected rewards given the states of the environment. In order to find the long-term relationship between states and actions, the RL agent must fundamentally find a balance between exploration (trying out different actions) and exploitation (making use of already-found optimal actions).

Formally, an RL agent interacts with an environment \mathcal{E} , through state s_t , reward r_t , and action a_t at time t . The framework is shown in Fig. 3. The agent then learns to maximize the total accumulated reward and returns $R_t = \sum_k \gamma^k \cdot r_{t+k}$, where $\gamma \in (0, 1]$ is a discount factor reflecting the value of future reward at present.

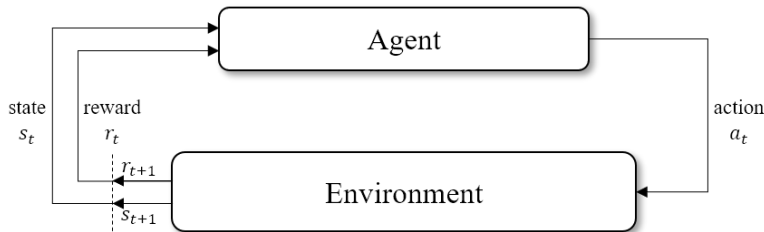


Figure 3. An RL agent interacts with an environment.

There are two categories in reinforcement learning frameworks depending on how an action is selected given a state. One through value approximation and the other is policy-based.

The action-value function, or Q-function, is the expected reward for selecting an action a_t in state s_t , and then follow policy π . Similarly, the value function is the expected reward from state s_t after following policy π . The Q-function and value function can be formally expressed as in Eq. (2) and Eq. (3) below, respectively. In the equations, θ^Q and θ^V represent parameters for the function approximators for the Q-function and value function, respectively.

$$Q^\pi(s, a; \theta^Q) = \mathbb{E}[R_t | s = s_t, a = a_t] \quad (2)$$

$$V^\pi(s; \theta^V) = \mathbb{E}[R_t | s = s_t] \quad (3)$$

Through iterative optimization, the Q or value function is updated and then used to derive the optimal action given the current state, as expressed in the equations below where P is the state transition probability.

$$\pi^*(s_t) = \operatorname{argmax}_{a \in A} Q^{\pi^*}(s_t, a; \theta^Q) \quad (4)$$

$$\pi^*(s_t) = \operatorname{argmax}_{a \in A} \sum_{s'} P(s' | s, a) \cdot V^{\pi^*}(s_t; \theta^V) \quad (5)$$

When using the Q function, a neural network is employed to approximate the value estimation and learn to reduce the value error for the following equations. Examples of the RL framework in this category are DQN and DDQN (Mnih et al., 2013; Mnih et al., 2015; Van et al., 2016).

$$L(\theta^Q) = E \left(r + \gamma \cdot \max_{a_{t+1}} Q(s_{t+1}, a_{t+1}; \theta^Q) - Q(s_t, a_t; \theta^Q) \right)^2 \quad (6)$$

Another category of RL frameworks is the policy gradient methods that work by estimating the policy gradient and updating parameters in the direction of increasing expected rewards J . With the policy gradient theorem, the most commonly used estimator has the form of Eq. (7).

$$\theta_{t+1} = \theta_t + \alpha \cdot \nabla \hat{J}(\theta_t) \quad (7)$$

$$\nabla J(\theta) = \mathbb{E}[\nabla \log \pi_\theta(a_t | s_t) \cdot \hat{A}_t] \quad (8)$$

where π_θ is a stochastic policy and \hat{A}_t is an estimation of the advantage function at each time step t . Here, the advantage is the gap between return and value estimation, which we will cover later in this paper. As in the value function-based reinforcement learning frameworks, the loss function shown in Eq. (8) plugged into the auto-differentiation software will find optimal parameters θ^* by minimization. A2C/A3C implements in parallel this approach with multiple instances of environments using the value function approximator as the baseline for the policy update (Mnih et al., 2016).

$$L^{PG}(\theta) = \mathbb{E}[\log \pi_\theta(a_t | s_t) \cdot \hat{A}_t] \quad (9)$$

It is empirically known that using this loss to optimize the parameters in multiple steps leads to a similar trajectory in the parameter space. However, doing so is not well justified, and sometimes fails to learn in the event of large policy updates within a single step (Schulman et al., 2017).

To address this problem, TRPO (Schulman et al., 2015) suggests a surrogate objective for the loss function. The following function is used to impose constraints on the size of the policy update based on the Trust-region theorem (Schulman et al. 2017).

$$\begin{aligned} & \max_{\theta} \mathbb{E} \left[\frac{\pi_\theta(a_t | s_t)}{\pi_{\theta_{old}}(a_t | s_t)} \cdot \hat{A}_t \right] \\ & \text{s.t. } \mathbb{E}[KL\{\pi_{\theta_{old}}(\cdot | s_t), \pi_\theta(\cdot | s_t)\}] \leq \delta \end{aligned} \quad (10)$$

Here, θ_{old} is the policy parameter before an update and KL is the Kuller-Liebler divergence, which represents the difference between two random distributions. Solving this optimization problem involves multi-step optimization procedures that require extensive computation and time. Therefore, TRPO suggests a relaxed version of the optimization problem as follows.

$$\max_{\theta} \mathbb{E} \left[\frac{\pi_{\theta}(a_t | s_t)}{\pi_{\theta_{old}}(a_t | s_t)} \cdot \hat{A}_t - \beta \cdot KL(\pi_{\theta_{old}}(\cdot | s_t), \pi_{\theta}(\cdot | s_t)) \right] \quad (11)$$

The equation above moves the constraint into the objective function as a penalty with a coefficient β . The loss function in TRPO is the surrogate function with a penalty. This significantly reduces the complexity of solving the optimization steps of the previous formulation.

However, the relaxed problem above still requires quite a large amount of computation for each step to run. Therefore, PPO (Schulman et al., 2017) suggests a rough approximated version of TRPO, as in the following equation.

$$L^{PPO}(\theta) = \mathbb{E}[\min(r_t(\theta) \cdot \hat{A}_t, \text{clip}(r_t(\theta), 1 - \epsilon, 1 + \epsilon) \cdot \hat{A}_t)] \quad (12)$$

$$r_t(\theta) = \frac{\pi_{\theta}(a_t | s_t)}{\pi_{\theta_{old}}(a_t | s_t)} \quad (13)$$

Here, the *clip* function bounds the input within $[1 - \epsilon, 1 + \epsilon]$. In PPO, instead of the heavy computation for calculating the penalty, the amount of update is bounded to some range, which greatly reduces computation time. The most important effect of the clipping loss is to prevent large destructive policy updates in a single update, which is the empirical problem of A2C.

In conjunction with an A2C style implantation and the generalized advantage estimator (GAE) (Schulman, Moritz et al. 2015), PPO has shown stable training performance in a wide range of reinforcement learning problems. This is why we used PPO as our main reinforcement learning framework in this study.

3. Topology Optimization by Deep Learning: TopOpNet

In this section, we elaborate on TopOpNet. TopOpNet approximates the topology optimization algorithm, which requires iterative and heavy matrix manipulations, requiring an extensive amount of computation power and time. To capture the underlying non-linearity of the algorithm, we used neural networks. The proposed neural network architectures show results similar to those of the algorithm in much less time. The time required to run the topology optimization algorithm is on the order of 10 min, whereas that of TopOpNet is less than 10 ms. Owing to the generalization characteristic of deep learning, TopOpNet sometimes shows better results in cases where the topology optimization algorithm fails to maintain symmetry.

3.1 Training and validating data

A total of 639 reference images were used. We divided the reference images into two sets: 500 for training and the rest for validation. The training set was used for training the network and the validating set was used for validating the training process and for testing the generalization performance of the algorithm after the training process.

As discussed in Section 2.1, two design parameters were chosen: similarity weight and force ratio. From now on, we will name similarity weight and force ratio c_1 and c_2 , respectively. The range of the parameters c_1 and c_2 were then fitted to the problem that we were addressing, the topology optimization of the wheel design. As a result, $c_1 \in [0.0005, 5.0]$ and $c_2 \in [0.0, 0.4]$. In order to generate the training and validating datasets, we sampled 11 points in the parameter space at equal distances. Due to its physical nature, we sampled c_1 in log-scale while linear-scale was used for c_2 . Therefore, in total, for one reference image, we applied 121 combinations of parameters.

We then derived the 121 resulting topology-optimized images from one reference image with the topology optimization algorithm. Hence, the inputs were a reference image I_{ref} , c_1 , c_2 , and the output was a topology-optimized image I_{opt} . Thereby, $I_{opt} = f(I_{ref}, c_1, c_2)$. With the precalculated datasets $(I_{ref}, c_1, c_2, I_{opt})$, we approximated the function f with a deep neural network.

3.2 Network Architectures

We propose two neural network architectures for the TopOpNet problem. As discussed, the inputs of the network were a reference image and the two optimization parameters (I_{ref}, c_1, c_2) , and the output was the

optimized image I_{opt} . The size of the image was regularized to 128×128 with a single channel, and the parameters were simply two floating numbers. The following methodology was devised to combine an image with two parameters.

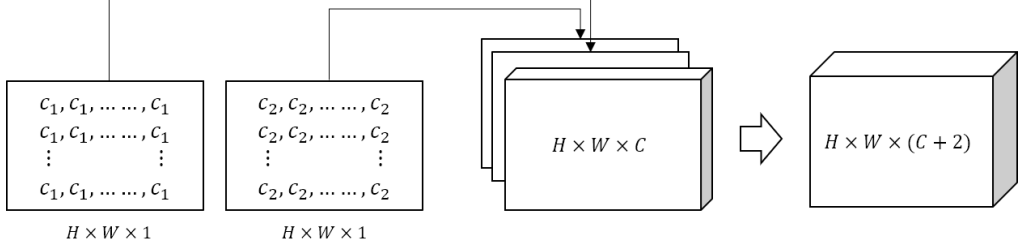


Figure 4. Parameter Concatenation Layer

Fig. 4 illustrates the parameter concatenating operation that we propose in this study. Given a tensor with shape $H \times W \times C$ where H , W , and C are height, width, and channel respectively, we repeated c_1 and c_2 to generate the same shape in height and width, only different in channel dimension. Then, we concatenated the two parameter layers on the tensor resulting in an increment on the channel dimension. We performed the parameter concatenation operations at the beginning of each layer to pass the information of the parameters.

3.2.1 Model A

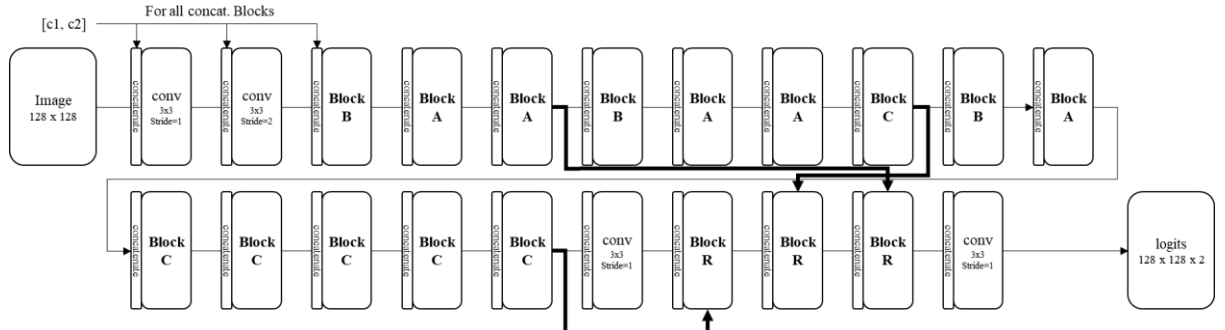
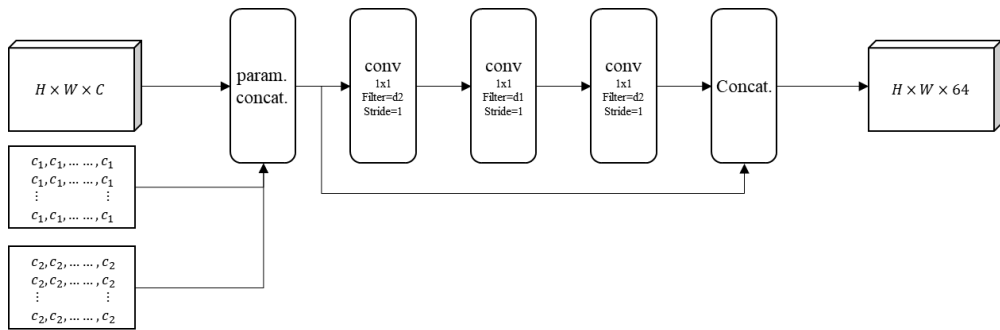


Figure 5. Model with ASPP (Model A).

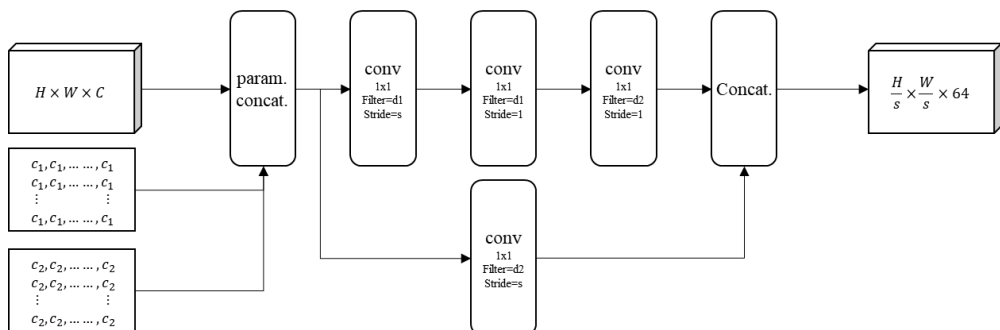
The first network architecture that we propose is based on the Inception (Szegedy et al., 2017) and FCN (Long et al., 2015) architectures with ASPP features. Fig. 5 shows the entire architecture of our first proposed model (Model A). The network architecture consists of mainly two sets of blocks: encoding blocks, and decoding blocks. The encoding part is a sequence of the blocks A, B, and C, each of which has its own inner network architecture, as shown in Fig. 6. Given an input tensor, the encoding part decreases the height and width of the input tensor by 8. The decoding part consists of three R blocks, each of which doubles the height and width of the input tensor. Thus, our architecture extracts features from the input tensor by $1/8$ and then reconstructs a topologically optimized design with the decoding part.

In order to help preserve the low-level features extracted within the encoding part, we also added three skip layers to pass the features to the decoding part. The skip layers are depicted with bold arrows in Fig. 5. Note that at the beginning of each block, we adopted a concatenated layer to incorporate the parameters c_1 and c_2 .

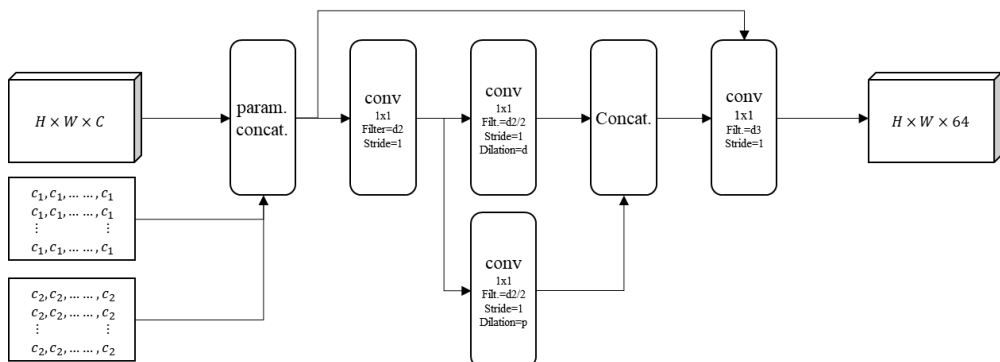
Fig. 6 shows the architecture of blocks A, B, and C. Note that only block B receives the stride as input, which is used to decrease the size of the feature map. By sequentially applying block C, we can construct an ASPP by increasing the dilation size. In block C, we split the feature map into two sets and apply different dilation sizes to capture features with different receptive field sizes. The total number of trainable parameters in model A were approximately 14 million, which is less than the network models used for semantic segmentation in ResNet, FCN, and Inception.



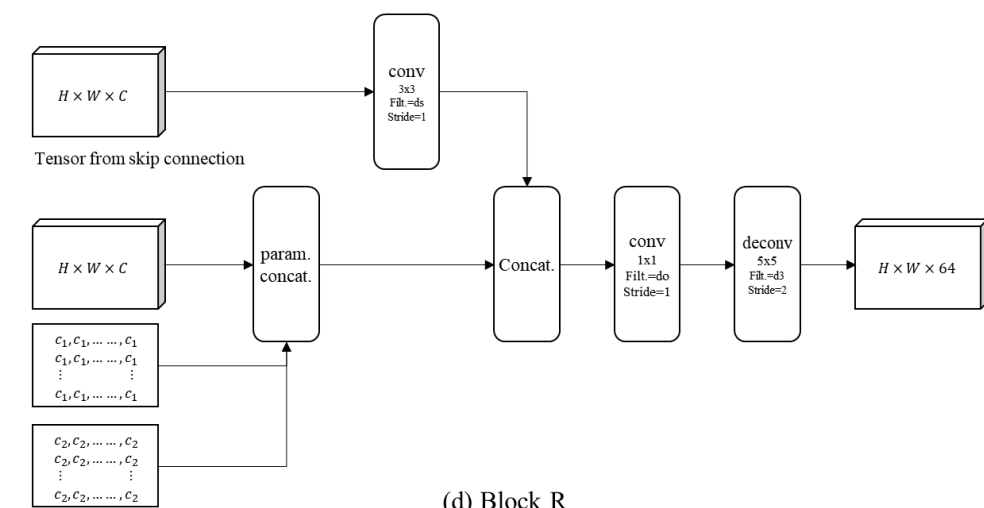
(a) Block A



(b) Block B



(c) Block C



(d) Block R

Figure 6. Blocks in model A.

3.2.2 Model B

The second model we used for TopOpNet, model B for simplicity, reduces the number of trainable parameters to boost the speed of training while slightly sacrificing performance. Fig 7 shows the overall architecture of model B. Similar to the previous model, the general architecture consists of encoding and decoding blocks. However, only one static block was used for each part in both the encoding and decoding blocks.

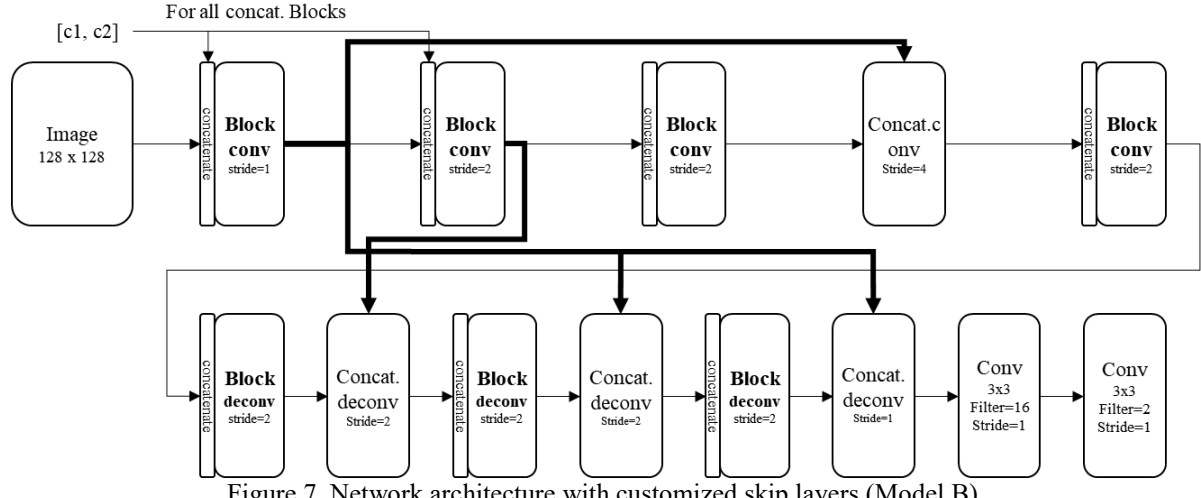
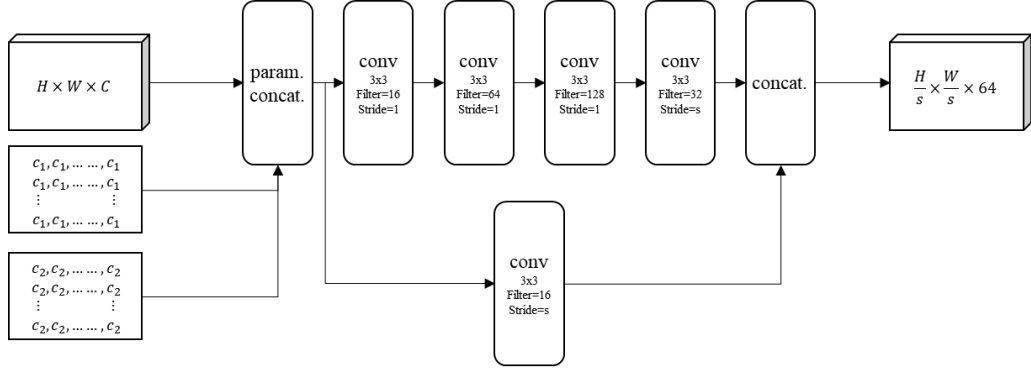
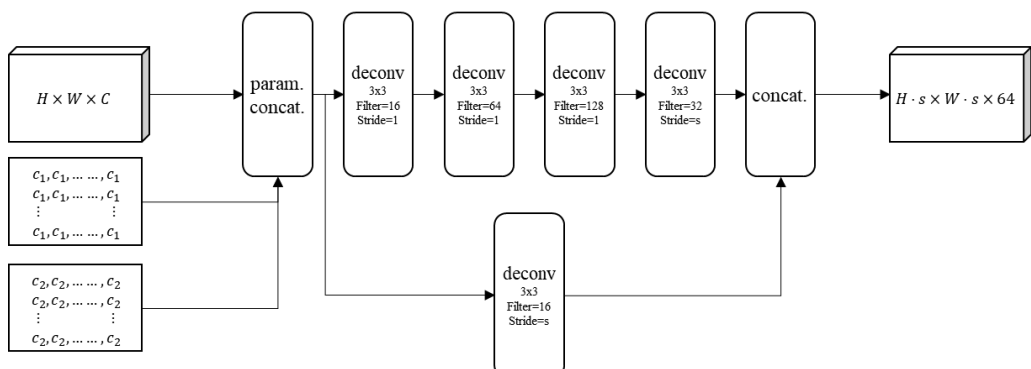


Figure 7. Network architecture with customized skip layers (Model B).

Fig. 8 shows the encoding and decoding blocks used in model B. The encoding block decreases the size of the input tensor by s using the stride size. It has a main stream of layers with a residual connection. Conversely, the decoding block has mainly deconvolution layers and enlarges the size of the input tensor by s using strides.



(a) Encoding block



(a) Decoding block

Figure 8. Encoding and decoding blocks in model B.

The number of parameters for this model was approximately 1.25 million, which is 1/10 of that of model A. Because our problem, approximating the topology optimization algorithm, is somewhat restricted due to the limited amount of data, this simplified model was considered as having good performance.

By trying many different combinations on the position of the skip networks, we found that the one proposed in the figure shows the best performance. This performance is presented in the following subsection.

3.3 Training

For training, we used the Adam optimizer (Kingma & Ba, 2017) with a learning rate of 0.0001 for both models. The size of the batch for training was 16; however, a larger batch is preferable if more memory is available on the GPU. As mentioned previously, we split 639 reference images into 500 training and 139 validating/testing images. We also applied regularization on the trainable variables with a regularization weight of 0.0001. The cross-entropy loss was used to calculate the loss.

In addition, in order to increase the generalization performance of the network, we augmented the input reference image in two ways. First, Gaussian noise was added to each pixel to add pixel-level noise, and the rotation of the reference images was randomly chosen within $[0, 359]$ degrees.

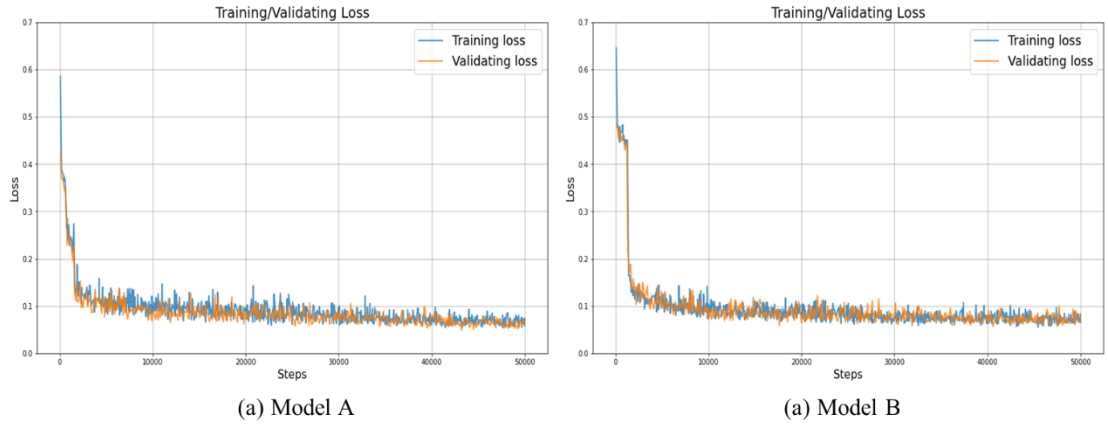


Figure 9. Training and validating loss during training.

As can be seen in Fig. 9, the training and validating losses show a similar trend, which indicates that the training was performed well without overfitting. Here, a training step consists of one forward and back propagation with one batch of training data.

3.4 Results

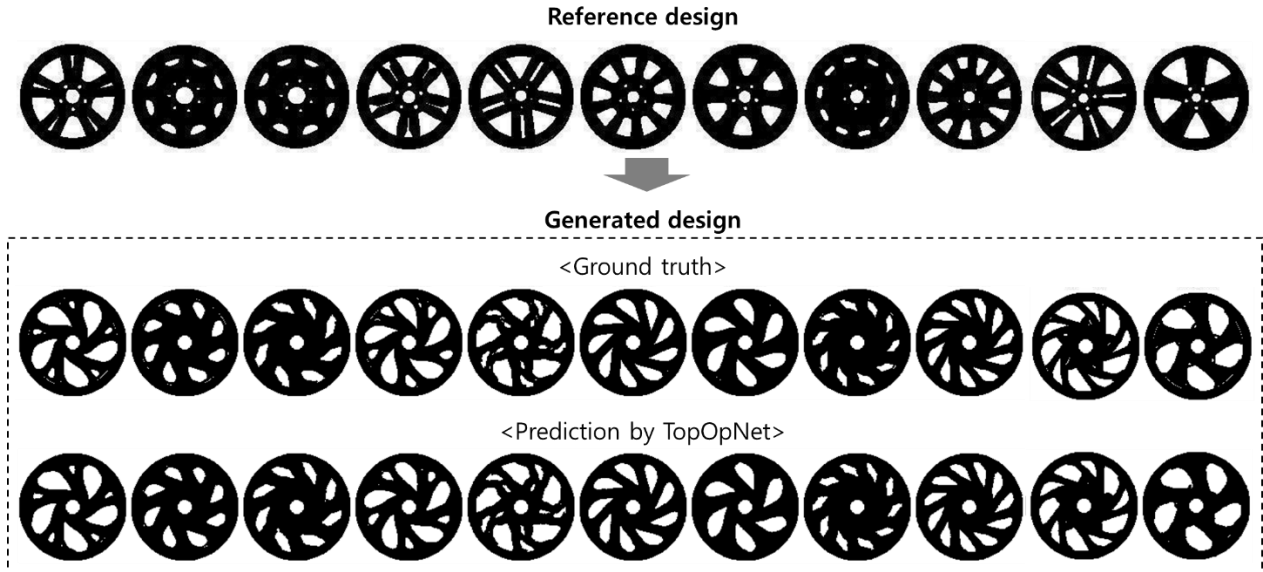


Figure 10. TopOpNet results, (top) reference design, (middle) ground truth, (bottom) prediction.

Fig. 10 shows the prediction results of the topology optimization. Because the results from models A and B were similar with minor errors, we only present the results of model A in this paper. However, the performances of the two models are compared later in this subsection.

As can be seen in the figure, the neural network approximates the topology optimization algorithm well in most cases. In some cases, the approximation is better, as shown in Fig. 11. We believe that the augmentations we applied on the training data result in better symmetry preservation in the results.

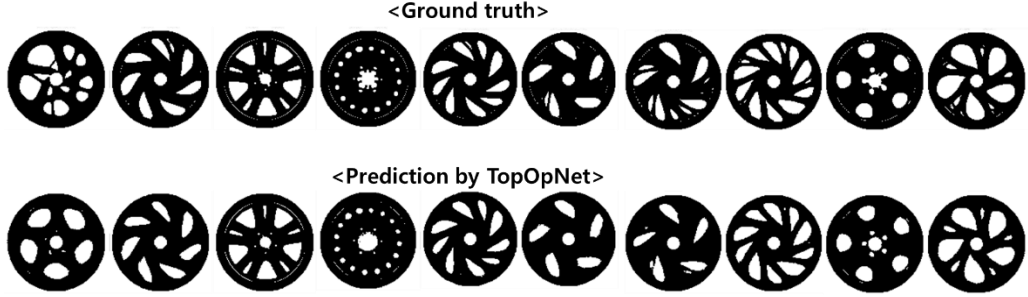


Figure 11. TopOpNet better results, (top) ground truth, (bottom) prediction.

Table 1 shows the performance comparison of the two network architectures proposed in this paper. Here, the cross-entropy, pixel difference, and intersection over union (IoU) metrics are compared. IoU is a metric mainly used in the field of object detection, it can measure how similar the generated designs are. In general, model A shows better performance by showing less cross-entropy, pixel difference, and higher IoU. In addition, model A shows more stable results by having less standard deviation. This is due to the greater learning capacity resulting from the additional trainable variables.

Table 1. Performance comparison of model A and B.

Model		Cross Entropy		Pixel Difference		IoU	
Models	Size (#params)	Mean	Std	Mean	Std	Mean	Std
Model A	14,630,412	0.038253	0.024770	0.015174	0.010706	0.969770	0.020152
Model B	1,250,214	0.046868	0.029488	0.017917	0.012569	0.964456	0.023409

In this section, we propose two network architectures for approximating the topology optimization algorithm. In general, the topology optimization algorithm is a CPU-intensive job that requires extensive matrix manipulation. The algorithm takes approximately the order of seconds for simple inputs. With our proposed approach and network architectures, the job can be run in less than ms on an NVidia Geforce 1080 Ti GPU. The huge reduction in time is exploited in the next task we address, finding the maximum diversity in designs with reinforcement learning.

4. Generative Design by Reinforcement Learning: GDNet

In this section, we address the problem of generating a set of diverse wheel designs using a reinforcement learning approach. In other words, proposing a set of parameters, $\{c_1^i, c_2^i\}, i \in \{1, 2, \dots, n\}$ produces a set of new designs with maximum diversity. In this section, we present the RL problem formulation and GDNet of the PPO agent. Then, data processing and training methods are presented, followed by the results. Note that applying RL is feasible through the reduced time for the topology optimization process with TopOpNet.

4.1 Problem Formulation

Fig. 12 shows the RL framework with GDNet. Here, the environment is the topology-optimization module, namely TopOpNet. Because RL requires multiple instances of the environment to gather more generalized and time-uncorrelated experiences, we implemented an environment with multiple TopOpNets within it. The TopOpNet module takes an image of size 128×128 and generates a topologically optimized image with the same size. While doing so, it employs the parameters c_1 and c_2 . Given an image and a parameter set, the TopOpNet module generates a single image. To generate a fixed number of output images, two sequences of parameters $\{c_1^i, c_2^i\}, i \in \{1, 2, \dots, n\}$ are defined as an action in a single episode. In our problem, the formulation n was set to 5 and all combinations were used to generate outputs resulting in 25 images. In order to simplify the problem without loss of generality, we split the parameter space into 11 discrete values for this problem formulation.

The generated images are used to derive a reward value, representing the diversity of the generated images, and passed to the RL agent as a state. The RL agent uses the reward and the state as inputs and generates an action that has two values for c_1 and c_2 . The generated action is then passed into the environment for the next step. Thus, in our problem formulation, an episode consists of 5 steps. At the end of an episode, the total diversity between the 25 resulting images is evaluated as the objective of the problem.

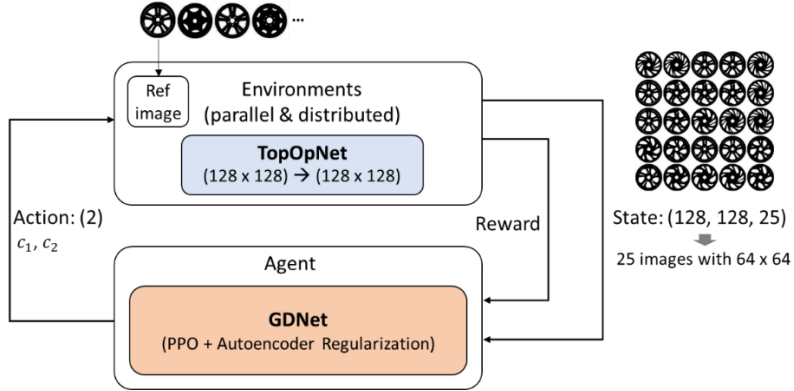


Figure 12. RL framework with GDNet

Therefore, at each time step, the agent generates an action of (c_1, c_2) , and then it is passed onto the environment. The environment then generates additional designs on top of the previous ones, as shown in Fig. 13. In the figure, the upper left squares show the positions of the generated images in the 5×5 grids, each axis corresponds to parameters c_1 and c_2 . The rest of the squares show the generated images for each time step. Here, we simply stacked the generated image instead of positioning it at the exact location as in the other figures. After 5 steps, the episode ends and the reward or diversity is evaluated for that episode.

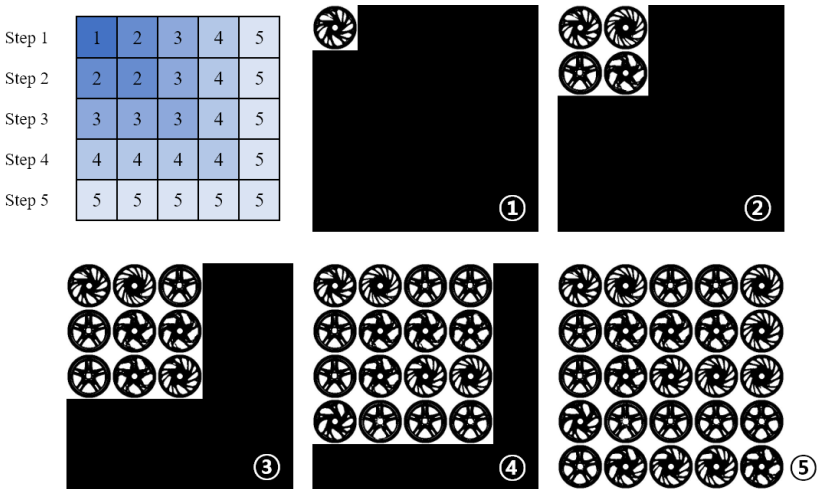


Figure 13. Sequential actions and states

In order to verify that our RL problem has a non-linear property and does not have a trivial solution, we searched the optimal parameter sets leading to the maximum diversity in designs with exhaustive search for a number of input images. Fig. 14 shows the optimal actions for two input reference images and the overlap of all optimal actions for a number of randomly selected inputs. As can be seen in the figure, in some cases, parameters other than the ones at the edges are solutions (middle 0.12 for c_2), which means the solutions are not trivial. The overlapping graph (right) shows that the answers have outstanding tendencies, but at the same time have different configurations for each reference input image.

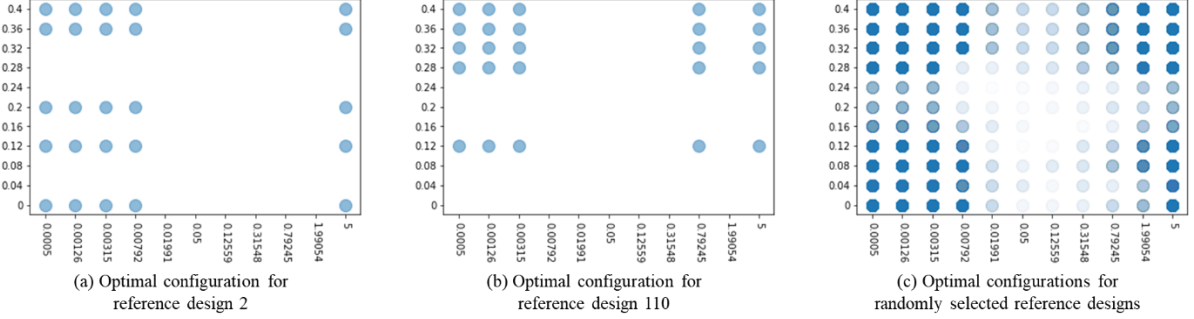


Figure 14. The optimal actions with exhaustive search.

The reward function must capture the diversity of the generated outputs. In this work, we applied two metrics for the diversity: pixel difference and structural dissimilarity (Wang et al., 2004). The pixel difference is basically the Euclidean distance between the two images. Let x_i represent the pixel value of an image i . Then, the sum of the L2 distance of x_i from all other images j , , is as shown in Eq. (14). Then, the average of the L2 norm of the pixel value for all images is as shown in Eq. (15). As it can be derived in the equation, the final value is the difference between the square mean of all values on that pixel subtracted by the square of all means. By the Cauchy-Schwarz inequality, the pixel difference on the pixel for all images is larger than 0. In Eq. (15), the $\frac{1}{2}$ accounts for the duplicated summation of the (i,j) and (j,i) pair. For simplicity of calculation, the pixel difference metric requires less time for its calculation, which is a suitable characteristic for reinforcement learning.

$$\begin{aligned} L_i &= \frac{1}{N} \sum_j (x_j - x_i)^2 \\ &= \frac{1}{N} \sum_j (x_j^2 - 2x_j x_i + x_i^2) \\ &= \frac{1}{N} \sum_j x_j^2 - \frac{2}{N} x_i \cdot \sum_j x_j + x_i^2 \end{aligned} \tag{14}$$

$$\begin{aligned} L &= \frac{1}{2N} \sum_i L_i \\ &= \frac{1}{2N} \sum_i \left(\frac{1}{N} \sum_j x_j^2 - \frac{2}{N} \cdot \sum_j x_j \cdot x_i + x_i^2 \right) \\ &= \frac{1}{2N} \left(N \cdot \frac{1}{N} \sum_j x_j^2 - 2 \cdot \frac{1}{N} \sum_j x_j \cdot \sum_j x_j + \sum_j x_j^2 \right) \\ &= \frac{1}{2} \left(\frac{1}{N} \sum_j x_j^2 - 2 \cdot \left(\sum_j x_j \right)^2 + \frac{1}{N} \sum_j x_j^2 \right) \\ &= \frac{1}{N} \sum_j x_j^2 - \left(\sum_j x_j \right)^2 \end{aligned} \tag{15}$$

On the other hand, structure dissimilarity takes windows of pixels $N_w \times N_w$. Eq. (17) shows the definition of the structural dissimilarity DSIM. In the equation, SSIM is the structural similarity, which represents the similarity of the two grids x and y . Here, μ_x, μ_y are the averages, σ_x, σ_y are the variances, and σ_{xy} is the covariance of x and y . k_1 a k_2 are constant values for stabilizing the division with a weak denominator. For our calculations, we used $N_w = 11$. In this case, the total reward is the average of the DSIM value for all pairs (N pairs) of the generated image, as shown in Eq. (18).

$$SSIM(x, y) = \frac{(2\mu_x\mu_y + k_1) \times (2\sigma_{xy} + k_2)}{(\mu_x^2 + \mu_y^2 + k_1) \times (\sigma_x^2 + \sigma_y^2 + k_2)} \tag{16}$$

$$DSIM(x, y) = \frac{1 - SSIM(x, y)}{2} \tag{17}$$

$$L = \frac{1}{N} \sum_{i,j} DSIM(i, j) \tag{18}$$

The two reward metrics were used as reward functions in our formulation and their performance was compared after training. Therefore, L for each reward metric was used to calculate the diversity of the generated image.

4.2 Structure of GDNet

The proposed PPO agent, GDNet, generates an action and an estimated value given a state with size $128 \times 128 \times 25$, as seen in Fig. 12. Because an action is a set of parameters, c_1 and c_2 are each one a set of 11 discrete values. Therefore, the shape of the output of the policy network is 2×11 , and that of the value network is a single value. As stated in the PPO paper (Schulman et al., 2017) we used a shared embedding architecture in which an encoder extracts embedding features from the input tensor and the embedding vector, which has a shape of 2048 and is fed into the policy and the value networks.

In addition to the basic network blocks, we also adopted a decoding network to decode the original inputs from the embedding vector. The decoding networks were inspired by the VAE (Variational Auto-Encoder) architecture (Kingma & Welling, 2013), which extracts features from the input and reconstructs the original inputs from the embedding vector. By doing so, VAE compresses the input data using an embedding vector. In our architecture, the encoding and decoding blocks correspond to the VAE, which enhances the feature extraction of the network. In other words, we used VAE as a regularizer for the network to avoid overfitting. The entire architecture of our PPO agent is shown in Fig. 15.

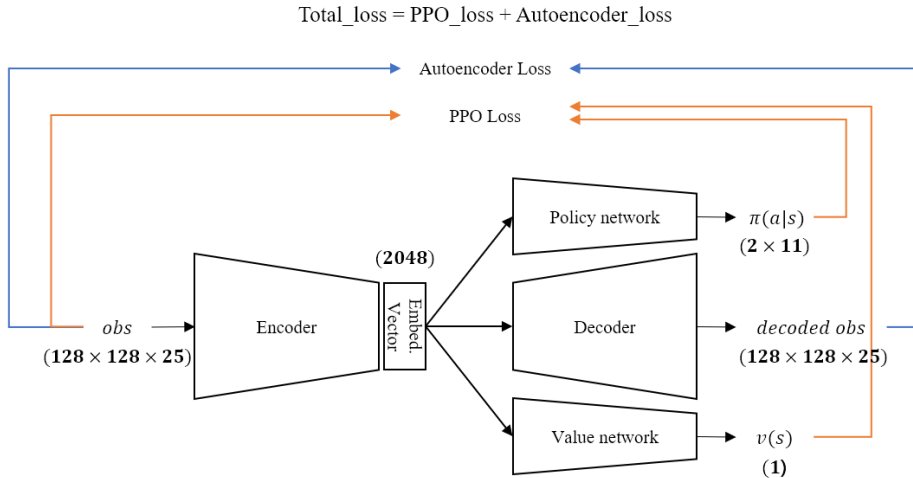


Figure 15. The PPO agent with VAE regularizer.

An encoder, decoder, policy, and value network for our agent can be constructed in many ways. We used a simple CNN with convolutional layers for the encoder and deconvolution layers for the decoder. For the policy and the value networks, we used simple multilayer perceptron (MLP) layers.

4.3 Training and Results

The PPO agent was then trained with 500 input images and the performance was measured with the remaining 139 images as in the case of the TopOpNet. To compare the performance of the two reward functions, we fixed the training step to 5,000, which corresponded to 1,000 episodes. To achieve time-uncorrelated experience, 64 simultaneous environments were created, each having a different input reference image. The PPO agent was trained after every 5 episodes with a learning rate of 0.0001. As for the range of the reward functions, we normalized the reward function so that the values were within the range $[-1.0, 1.0]$.

Fig. 16 shows the training loss and reward values during training with the pixel difference reward function. As can be seen in the figure, the reward saturates near 0.6, and the loss near 0.002.

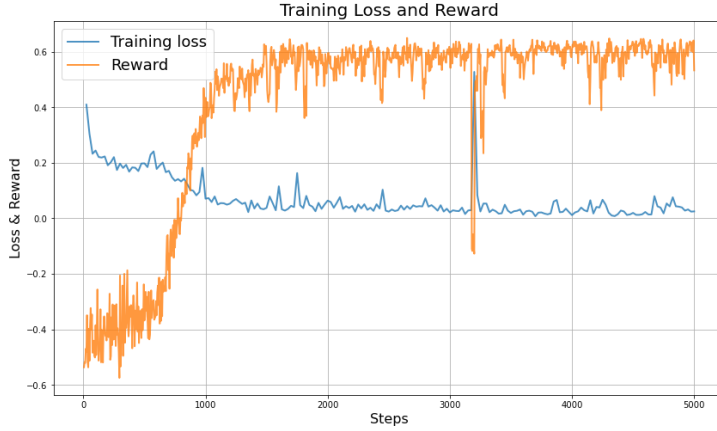


Figure 16. Training loss and reward during training with pixel difference reward.

The test results are shown in Fig. 17. The figure compares the resulting designs from GDNet (RL-learned) with one with equal distance action (equ-distance). Here, the equal-distance action is a set of actions having the same gap between each pair of elements in a c_1, c_2 space. Diversity can also be evaluated by the number of final available designs. For this, we eliminated designs that were similar to others by measuring the L1 distance between each pixel. If the two designs had 97% similar pixel values, one of the designs was eliminated. In the figure, the eliminated designs are shown in gray.

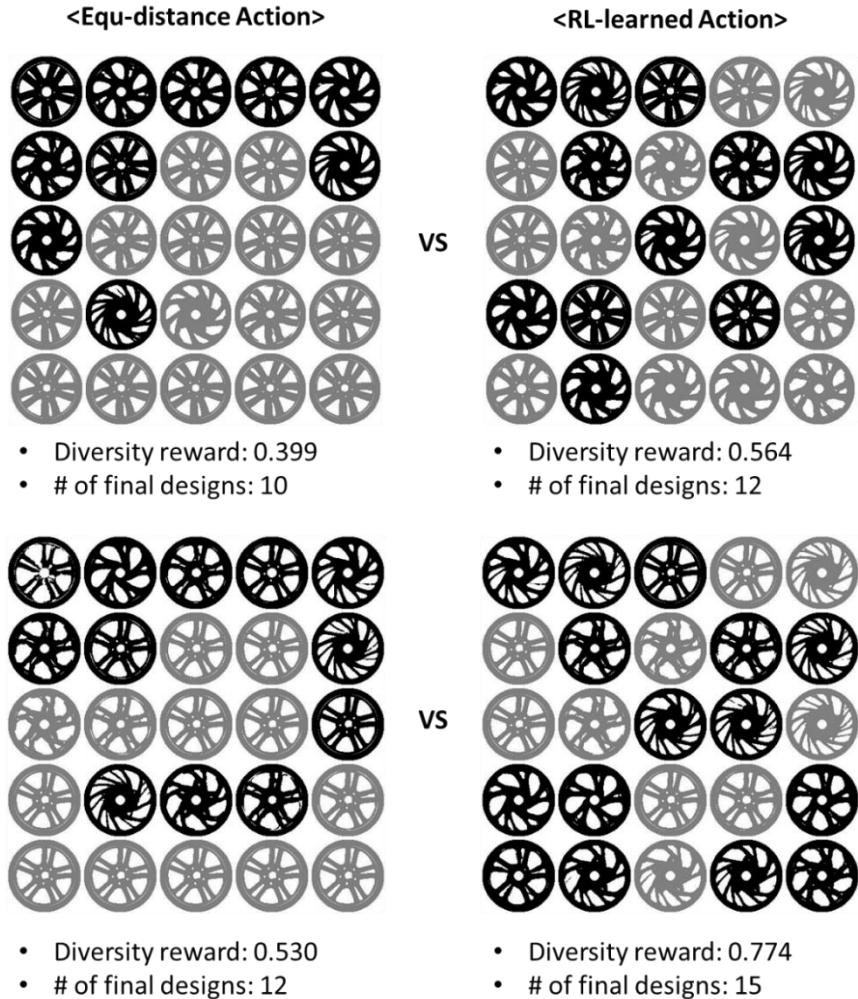


Figure 13. Test samples: comparison between equ-distance and RL-learned actions

As expected, the reward, representing the diversity of the designs, increased when using RL-learned actions. The overall comparison over the entire testing dataset is presented in Table 2. The diversity reward and the number of final designs were increased in 39.9% and 11.5%, respectively. The diversity reward and the number of final designs showed statistically significant differences between equ-distance and RL learning actions, at $p < 0.001$. This is intrinsically explainable because our objective was to maximize diversity.

Table 2. Comparison of testing dataset

	Diversity reward (pix-diff)		# of final designs	
	Mean	Std	Mean	Std
Action	Equ-distance	0.431	0.11	10.12
	RL-learned	0.603	0.14	11.28*

Additionally, we also tried the A2C framework (Mnih et al., 2016). However, we were unable to observe trained results with many different combinations of hyper-parameters. We believe that the clipping-based surrogate loss of the PPO framework contributes to the training performance in our problem formulation, while vanilla A2C cannot.

As stated above, we trained the network with 500 input images and evaluated the performance of the model with the remaining 139 images. In most cases, 5,000 training steps were sufficient to reach a stable convergence point. Using the same settings, we trained the same model with each reward function and evaluated the performance using both reward metrics. Table 3 shows the evaluation results. The X-axis represents the reward function for testing and the Y-axis for training.

Table 3. Evaluation results for training and testing reward functions

Reward function	Test results		
	Pixel difference		Structural dissimilarity
	Pixel difference	0.603	0.159
Structural dissimilarity		0.426	0.130

As can be seen in the table, when trained with pixel difference reward, the performance of the model outperforms the other models. Thus, we find that the pixel difference reward is more suitable for our problem.

5. Conclusion

This study addresses the generative design problem with a deep neural network. An RL-based generative design framework is proposed to determine the optimal combination of design parameters that can maximize the diversity of generated designs. An automotive wheel design case study demonstrated that the proposed framework can find the optimal design parameter combinations based on given reference designs. For the proposed framework, two deep neural networks were developed as follows.

First, we approximated the time-demanding and computation-intensive topology optimization algorithm for the wheel design using a deep neural network, which we call TopOpNet. With our two proposed network architectures, topology optimization can be computed within an order of milliseconds (an inferencing time), while the algorithm requires an order of 10 min in general. This, in turn, leads to the GPU processing the data, not the CPU. The network architectures have similar components used in semantic segmentation, and we optimized the architectures for our problem.

Second, taking advantage of the reduced computation time of TopOpNet, we tackle the maximum generative design diversity problem using the reinforcement framework, GDNet. We first found that the problem has non-linear characteristics so that deep learning was a suitable solution. Then, the problem was formulated as a sequential process, suggesting a set of parameters at each step so that the reinforcement framework could be applied. We used VAE regularizing as a means to accelerate the training process by helping the network extract more diverse features. PPO has shown stable training results while others have not.

RL-based generative design has the potential to suggest diverse designs and we plan to extend the approach to other design problems in the future.

Acknowledgement

This work was supported by National Research Foundation of Korea (NRF) grants funded by the Korean government [grant numbers 2017R1C1B2005266, 2018R1A5A7025409]. The authors would like to thank Yebin Youn for her help in optimizing the model architecture.

References

Andreassen, E., Clausen, A., Schevenels, M., Lazarov, B. S., & Sigmund, O. (2011). Efficient topology optimization in MATLAB using 88 lines of code. *Structural and Multidisciplinary Optimization*, 43(1), 1-16.

Banga, S., Gehani, H., Bhilare, S., Patel, S., & Kara, L. (2018). 3d topology optimization using convolutional neural networks. *arXiv preprint arXiv:1808.07440*.

Chen, L. C., Papandreou, G., Kokkinos, I., Murphy, K., & Yuille, A. L. (2017). Deeplab: Semantic image segmentation with deep convolutional nets, atrous convolution, and fully connected crfs. *IEEE transactions on pattern analysis and machine intelligence*, 40(4), 834-848.

Ha, D. (2019). Reinforcement learning for improving agent design. *Artificial life*, 25(4), 352-365.

He, K., Zhang, X., Ren, S., & Sun, J. (2016). Deep residual learning for image recognition. In *Proceedings of the IEEE conference on computer vision and pattern recognition* (pp. 770-778).

Keshavarzzadeh, V., Kirby, R. M., & Narayan, A. (2020). Stress-based topology optimization under uncertainty via simulation-based Gaussian process. *Computer Methods in Applied Mechanics and Engineering*, 365, 112992.

Kingma, D. P., & Ba, J. (2014). Adam: A method for stochastic optimization. *arXiv preprint arXiv:1412.6980*.

Kingma, D. P., & Welling, M. (2013). Auto-encoding variational bayes. *arXiv preprint arXiv:1312.6114*.

Kirillov, A., He, K., Girshick, R., Rother, C., & Dollár, P. (2019). Panoptic segmentation. In *Proceedings of the IEEE conference on computer vision and pattern recognition* (pp. 9404-9413).

Krizhevsky, A., Sutskever, I., & Hinton, G. E. (2012). Imagenet classification with deep convolutional neural networks. In *Advances in neural information processing systems* (pp. 1097-1105).

Li, K., & Malik, J. (2016). Learning to optimize. *arXiv preprint arXiv:1606.01885*.

Lin, C. Y., & Lin, S. H. (2005). Artificial neural network based hole image interpretation techniques for integrated topology and shape optimization. *Computer methods in applied mechanics and engineering*, 194(36-38), 3817-3837.

Long, J., Shelhamer, E., & Darrell, T. (2015). Fully convolutional networks for semantic segmentation. In *Proceedings of the IEEE conference on computer vision and pattern recognition* (pp. 3431-3440).

Mnih, V., Badia, A. P., Mirza, M., Graves, A., Lillicrap, T., Harley, T., ... & Kavukcuoglu, K. (2016, June). Asynchronous methods for deep reinforcement learning. In *International conference on machine learning* (pp.

1928-1937).

Mnih, V., Kavukcuoglu, K., Silver, D., Graves, A., Antonoglou, I., Wierstra, D., & Riedmiller, M. (2013). Playing atari with deep reinforcement learning. *arXiv preprint arXiv:1312.5602*.

Mnih, V., Kavukcuoglu, K., Silver, D., Rusu, A. A., Veness, J., Bellemare, M. G., ... & Petersen, S. (2015). Human-level control through deep reinforcement learning. *nature*, 518(7540), 529-533.

Oh, S., Jung, Y., Lee, I., & Kang, N. (2018, August). Design automation by integrating generative adversarial networks and topology optimization. In International Design Engineering Technical Conferences and Computers and Information in Engineering Conference (Vol. 51753, p. V02AT03A008). American Society of Mechanical Engineers.

Oh, S., Jung, Y., Kim, S., Lee, I., & Kang, N. (2019). Deep generative design: Integration of topology optimization and generative models. *Journal of Mechanical Design*, 141(11).

Roux, W., Yi, G., & Gandikota, I. (2020). A spatial kernel approach for topology optimization. *Computer Methods in Applied Mechanics and Engineering*, 361, 112794.

Schulman, J., Levine, S., Abbeel, P., Jordan, M., & Moritz, P. (2015, June). Trust region policy optimization. In International conference on machine learning (pp. 1889-1897).

Schulman, J., Moritz, P., Levine, S., Jordan, M., & Abbeel, P. (2015). High-dimensional continuous control using generalized advantage estimation. *arXiv preprint arXiv:1506.02438*.

Schulman, J., Wolski, F., Dhariwal, P., Radford, A., & Klimov, O. (2017). Proximal policy optimization algorithms. *arXiv preprint arXiv:1707.06347*.

Sosnovik, I., & Oseledets, I. (2017). Neural networks for topology optimization. *arXiv preprint arXiv:1709.09578*.

Sun, H., & Ma, L. (2020). Generative Design by Using Exploration Approaches of Reinforcement Learning in Density-Based Structural Topology Optimization. *Designs*, 4(2), 10.

Sutskever, I., Vinyals, O., & Le, Q. V. (2014). Sequence to sequence learning with neural networks. In *Advances in neural information processing systems* (pp. 3104-3112).

Sutton, R. S., & Barto, A. G. (2018). *Reinforcement learning: An introduction*. MIT press.

Szegedy, C., Ioffe, S., Vanhoucke, V., & Alemi, A. A. (2017, February). Inception-v4, inception-resnet and the impact of residual connections on learning. In *Thirty-first AAAI conference on artificial intelligence*.

Szegedy, C., Liu, W., Jia, Y., Sermanet, P., Reed, S., Anguelov, D., ... & Rabinovich, A. (2015). Going deeper with convolutions. In *Proceedings of the IEEE conference on computer vision and pattern recognition* (pp. 1-9).

Van Hasselt, H., Guez, A., & Silver, D. (2016, March). Deep reinforcement learning with double q-learning. In *Thirtieth AAAI conference on artificial intelligence*.

Vaswani, A., Shazeer, N., Parmar, N., Uszkoreit, J., Jones, L., Gomez, A. N., ... & Polosukhin, I. (2017). Attention is all you need. In *Advances in neural information processing systems* (pp. 5998-6008).

Wang, Z., Bovik, A. C., Sheikh, H. R., & Simoncelli, E. P. (2004). Image quality assessment: from error visibility to structural similarity. *IEEE transactions on image processing*, 13(4), 600-612.

Yonekura, K., & Hattori, H. (2019). Framework for design optimization using deep reinforcement learning. *Structural and Multidisciplinary Optimization*, 60(4), 1709-1713.

Yoo, S., Lee, S., Kim, S., Hwang, K. H., Park, J. H., & Kang, N. (2020). Integrating Deep Learning into CAD/CAE System: Case Study on Road Wheel Design Automation. *arXiv preprint arXiv:2006.02138*.

Yu, Y., Hur, T., Jung, J., & Jang, I. G. (2019). Deep learning for determining a near-optimal topological design without any iteration. *Structural and Multidisciplinary Optimization*, 59(3), 787-799.